

Cr doped ZnO-graphene nanocomposite: one pot room temperature synthesis, characterization and antibacterial activity on mesophilic bacterial cells

Atanu Naskar, Hasmat Khan, Sunirmal Jana *

¹Sol-Gel Division, CSIR-Central Glass and Ceramic Research Institute, 196 Raja S.C. Mullick Road, Jadavpur, Kolkata 700032, India

*corresponding author e-mail address: sjana@cgeri.res.in, janasunirmal@hotmail.com

ABSTRACT

Present work reports for the first time on one pot, hydrazine mediated synthesis of Cr doped-ZnO-graphene (CZG) nanocomposites by adopting solution technique at room temperature varying chromium content (upto 10% Cr with respect to Zn) in the precursors. X-ray diffraction (XRD) and transmission electron microscopic (TEM) studies confirmed the presence of ZnO nanoparticles (NPs) of the nanocomposites. Reduction in crystallite size of ZnO with Cr doping was confirmed from XRD study. TEM micrograph also showed the uniform distribution of ZnO over reduced graphene oxide (rGO). The existence of chemical interaction/complexation between the available oxygen functionalities of rGO with the inorganic moieties ($\text{ZnO}/\text{Zn}^{2+}$) of CZG samples confirmed by FTIR, Raman, and UV-Visible spectroscopic analyses. The antibacterial activity was measured on *Escherichia coli*, *Pseudomonas aeruginosa*, *Staphylococcus aureus* and *Bacillus subtilis* to confirm the efficiency of the nanocomposite towards killing the bacterial cells. Among the nanocomposites, 5% Cr doped sample showed excellent antibacterial activity against the microorganisms.

Keywords: Doped ZnO nanoparticles; graphene, nanocomposite; room temperature solution process; antibacterial activity.

1. INTRODUCTION

Human beings are always trying to live in a healthy and hygienic environment. So, scientific research towards well being of human can always be the center of attention. Right now, the use of antibacterial agents is one of them which are taking the pivotal role for well being of human beings. The special ability of bacteria among the smallest living beings in the world is that it can develop and reproduce themselves due to their favorable structures as well as the presence of organelles [1]. They can also spread infectious agents in poor air circulation condition. Among the bacteria cells, mesophilic bacteria cells grow best in moderate to warm temperatures that range from 15 – 40 °C. In general, the antibacterial activity of a compound can be defined as to kill bacteria cells without harming the surrounding living cells [2]. The antibacterial compounds/agents can be either organic or inorganic material. However, the inorganic antibacterial material seems to be highly preferred over organic as they are highly stable at high temperature and pressure [1]. Till date, nanomaterials have shown the most effective antibacterial activity due to their unique physicochemical properties owing to large surface to volume ratios [3]. Other advantageous properties such as low toxicity to human cells, greater selectivity, stability in physiochemical solutions and chemical stability can also be considered for their use in human cells. Among the nanomaterials, metal oxide nanoparticles play a crucial role in exhibiting antibacterial activity due to their ability to disrupt the bacterial cell wall and kill them by accumulating in the cytoplasm or in the periplasmic region [2]. ZnO, one of most common metal oxide in nano dimension can be a good antibacterial agent. Use of ZnO in biological cells is also highly feasible as it has UV blocking capability, cost effective and has a wide range of antibacterial activity towards both Gram-positive and Gram-negative bacteria [4]. In brief, ZnO is biocompatible but it can selectively kill bacterial cells. ZnO is a

good antibacterial agent but its efficacy in the pristine stage is not good enough [2]. Therefore, an obvious challenge is that how to improve the antibacterial activity (AA) of ZnO. AA can be improved by introducing surface defects towards changing the visible absorption characteristics of the material [1]. In this respect, suitable doping of metal ions is one of the effective ways to introduce a surface defect in ZnO. A small amount of dopants (donors or acceptors) can influence a significant change in surface defects of ZnO crystal lattice [5]. The surface defects may shift the optical absorption towards the visible region and this can lead to giving an improved antibacterial activity of the material [1]. A plenty of research has already been done for the improvement of antibacterial activity of ZnO by Ag, Cu, Mg, Ce, Nd, Co, Y etc. doping [5]. However, the doping with transition metal chromium, (Cr) may be really fruitful for improving antibacterial activity. This is because chromium shows high biological factor compares to other transition metals [1]. It is worthy to mention that the ionic radius of Cr^{3+} ion is less than Zn^{2+} . This suggests that incorporation of Cr^{3+} ions can easily be made into ZnO crystal [5]. Reduced graphene oxide (rGO) is also an excellent biocompatible material due to its unique physiochemical properties such as large surface area, easy to functionalize with other materials including metal oxides [6] and it has high biocompatibility. The antibacterial activity of rGO has also been explored to reveal that it can directly influence to kill the bacterial cell [2]. It can also help the nanoparticles by playing the role of the matrix which can stabilize the nanoparticles to mitigate agglomeration problem [7]. Due to biocompatibility, a nanocomposite of ZnO-graphene can also be used for other biomedical applications [6]. Moreover, there are plenty of reports that found on ZnO-graphene [2, 3], Cr doped ZnO [1] for the study of antibacterial activity of the materials. To

the best of our knowledge, no report is available on the antibacterial activity of Cr doped ZnO-rGO nanocomposite.

Herein, we report for the first time, a facile pH, precursor concentration, and solvent dependent Cr doped ZnO-rGO nanocomposite synthesized at room temperature with the help of hydrazine hydrate by using optimized contents of zinc nitrate

2. EXPERIMENTALS

2.1. Synthesis of ZnO (ZO), ZnO-rGO (ZG) and Cr doped ZnO-rGO nanocomposite (CZG). Graphene oxide (GO) was synthesized by a modified Hummer's method as reported in our previous works [6]. In the present work, a fixed amount (50 mg) of as-synthesized GO was uniformly dispersed in deionized water (50 ml) by ultrasonication for about 2 h duration. In another solution, 0.1 M of zinc nitrate hexahydrate ($(\text{Zn}(\text{NO}_3)_2 \cdot 6\text{H}_2\text{O}$, Merck) and chromium nitrate ($\text{Cr}(\text{NO}_3)_3$ nonahydrate Sigma-Aldrich, 99%) of different contents (0, 2, 5, and 10 atomic percent, at%) with respect to Zn were uniformly dispersed in 50 ml of deionized water by continuous stirring. Accordingly, the synthesized nanocomposite products were named as ZG, CZG2, CZG5 and CZG10. Further, the GO dispersed in deionized water was mixed with zinc nitrate and chromium nitrate solutions while stirring continuously for 1 h to form stable precursors. Subsequently, hydrazine hydrate ($\text{H}_6\text{N}_2\text{O}$, Merck, 99-100%) was

hexahydrate, graphene oxide and chromium nitrate nonahydrate. To examine the antibacterial activity of the nanocomposite, Gram-negative (*Escherichia coli*, *Pseudomonas aeruginosa*) and Gram-positive (*Staphylococcus aureus*, *Bacillus subtilis*) bacteria have been utilized. It is noted that the Cr-ZnO-rGO nanocomposite shows an excellent antibacterial activity in most of the bacteria.

added in drop-wise (flow rate, 200 $\mu\text{l/s}$) manner for 5 s to the individual precursor solution and followed by sonicated (Piezo-U-Sonic ultrasonic cleaner) the aliquot for about 10 min. The pH of the aliquot became 2.20. A brown precipitation was seen at the bottom of the solution. After further addition of hydrazine and followed by sonication (10 min) in a similar manner, the pH of the medium reached 3.90. The same process was repeated till the medium pH became 8. The precipitate was then separated out by centrifugation and the resulting products were washed with deionized water and ethanol and centrifuged the products for several times. Finally, the centrifuged precipitate was dried in an air oven at $\sim 60^\circ\text{C}$ for 24 h. Similar procedures were followed for synthesis of ZnO-rGO nanoparticles (ZG) without using chromium nitrate and ZnO nanoparticles (ZO) where chromium nitrate and GO were not used.

3. CHARACTERIZATIONS

3.1 Materials. X-ray diffractometer (Bruker D8 Advance with DAVINCI design X-ray diffraction unit) with nickel filtered CuK_α radiation source ($\lambda = 1.5418 \text{ \AA}$) was used to measure X-ray diffraction (XRD) patterns of the samples in the 2θ range, $5^\circ - 80^\circ$. Raman spectra of graphene based samples (ZG and CZG10 along with precursor GO) were recorded from micro-Raman (Renishaw winVia Raman microscope) with an argon ion laser of an incident wavelength of 514 nm, an excitation source. FTIR spectral study was carried out by using Thermo Electron Corporation, USA makes FTIR spectrometer (Nicolet 5700). For each experiment, the number of scans was fixed at 100 with a wavenumber resolution of 4 cm^{-1} . To analyze the morphology and microstructure of the samples, a field emission scanning electron microscope (FESEM and FESEM-EDS, ZEISS, SUPRATM 35VP) was used. On the other hand, transmission electron microscopy (TEM) measurement of the samples was done by FEI Company made (Tecnai G2 30.S-Twin, Netherlands) machine at an accelerating voltage of 300 kV. Carbon coated 300 mesh Cu grids were used for the placement of the samples. Moreover, diffused reflectance method was adopted for measuring absorption spectra of the samples using an UV-VIS-NIR spectrophotometer (UV3600, Shimadzu, Japan) with ISR 3600 attachment.

3.2. Bacterial strains. Gram-positive bacteria (*Staphylococcus aureus*, ATCC 25923 and *Bacillus subtilis*, MTCC 2396) and Gram-negative bacteria (*Escherichia coli*, MTCC 2939 and *Pseudomonas aeruginosa*, MTCC 2453) were used in this work as

4. RESULTS AND DISCUSSION

4.1. Materials properties. 4.1.1. X-ray diffraction (XRD) analysis. X-ray diffraction patterns of as-synthesized graphene

the model microorganisms. Muller-Hinton-Broth (MHB) medium was used for the growth of bacteria. A single colony of bacteria (*E. coli/P. aeruginosa/S. aureus/B. subtilis*) was transferred to Muller Hinton broth (MHB) and incubated at 37°C until the density of the broth (containing the suspended organisms) reached the desired standard (0.5 McFarland standards) using sterile distilled water [2]. The organism suspension was used for further application within 30 min duration of the preparation.

3.3. Determination of minimum inhibitory concentration (MIC). The antibacterial experiment was carried out with Gram-positive bacteria - *Staphylococcus aureus* (*S. aureus*, ATCC 25923), *Bacillus subtilis* (*B. Subtilis*, MTCC 2396) and Gram-negative bacteria - *Escherichia coli* (*E. coli*, MTCC 2939), *Pseudomonas aeruginosa* (MTCC 2453) as the model microorganisms. MHB medium was used for the growth of bacteria. An approximately 10^7 cfu ml^{-1} *E. coli/P. aeruginosa/S. aureus/B. subtilis* bacteria cells were grown in 15 ml liquid MHB medium supplemented with different concentrations (1.5625, 3.125, 6.25, 12.5, 25, 50, 100, 200 $\mu\text{g ml}^{-1}$) of samples (ZO, ZG, CZG2, CZG5, CZG10) and incubated at 37°C . After that, the bacterial growth rate was investigated by optical density analysis where optical density (OD) of the treated and untreated bacteria (control) was measured at 600 nm using UV-Visible spectrophotometer (SpectraMax M5) after 24 h. Then, the results were further analyzed to check the antibacterial activity in terms of the MIC value.

oxide (GO), pristine ZnO (ZO), ZnO-rGO (ZG) and Cr doped ZnO-rGO (CZG) nanocomposites are shown in Figure 1. A strong

diffraction peak (2θ) appeared at $\sim 10.1^\circ$ with a relatively weak intensity XRD peak noticed at $\sim 42.4^\circ$ correspond to the crystal planes at (002) and (100) of GO [2]. However, these peaks of GO were disappeared after dropwise addition of hydrazine followed by ultrasonication in ZG, CZG2, CZG5, and CZG10 nanocomposite samples. The transformation of GO to rGO could be the reason for this result [8]. FTIR and Raman spectral studies of the samples (discussed later) were further carried out to confirm the transformation.

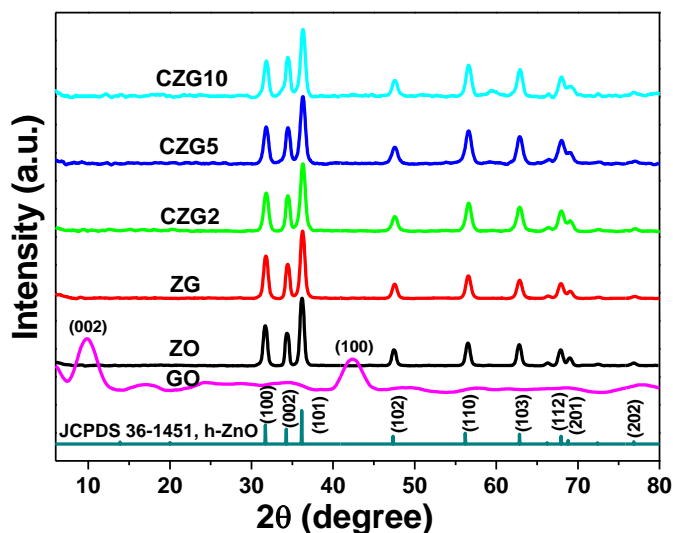


Fig. 1. XRD patterns of ZO, ZG, CZG2, CZG5 and CZG10 samples along with as-synthesized graphene oxide (GO).

It can clearly be seen from the **Figure 1** that, the XRD diffraction peaks of ZO, ZG, CZG2, CZG5 and CZG10 samples were fully matched with hexagonal ZnO (h-ZnO) [JCPDS 36-1451] as reported in our previous work [2, 3]. No other peaks except the ZnO peaks further prove the purity of the samples. A slight shift in 2θ values ($\sim 0.13^\circ$) towards higher diffraction angles was observed which implied the successful incorporation of Cr into ZnO crystal lattice. Due to the smaller ionic radius of Cr^{3+} (0.63 \AA) compared to Zn^{2+} (0.74 \AA), Cr^{3+} ions could easily substitute Zn^{2+} in the ZnO lattice without changing the crystal structure [5]. The average crystallite size (D) of ZnO crystallites was measured along (101) crystal plane by using Debye-Scherrer's equation (1).

$$D = k\lambda / \beta \cos\theta \quad (1),$$

where k is the proportionality constant ($k = 0.89$), λ is the wavelength of X-ray (1.5418 \AA), β is the FWHM (full width at half maximum) of the peak of maximum intensity in radians, θ is the diffraction angle and D is the crystallite size.

Using the equation (1), the measured ' D ' values of ZnO in pristine ZnO (ZO), ZG, CZG2, CZG5 and CZG10 nanocomposites were $\sim 25 \text{ nm}$, $\sim 19.5 \text{ nm}$, $\sim 14.5 \text{ nm}$, $\sim 13.5 \text{ nm}$ and $\sim 12 \text{ nm}$, respectively. Thus, the crystallite size of ZnO decreased in ZG nanocomposites with increasing Cr-doping concentration in the precursor solutions. The decrease in D of ZG with respect to ZO could be due to the large surface area of rGO that could prevent the grain growth [9]. There was further decrease of ZnO crystallite size in chromium doped ZG nanocomposites which confirmed the substitution of Cr^{3+} ions in Zn^{2+} of ZnO crystal lattice. The smaller crystallite size of ZnO could result in enhance surface area of the

nanocomposite which might contribute towards better antibacterial activity.

4.1.2. Morphology and microstructure. TEM analysis was performed on a representative sample CZG10 and the result is shown in Figure 2. The ZnO nanoparticles over rGO layer are distinctly visible in the TEM (Fig. 2a) image of the sample. The corresponding HRTEM image (Fig. 2b) shows the distinct lattice fringes with an interplanar distance of 0.28 nm , indexed to (100) plane of hexagonal ZnO. Therefore, the result is fully corroborated with the XRD data (Fig. 1) and confirmed the formation of ZnO nanoparticle in Cr-doped nanocomposite. Figure 2c displays the TEM-EDX spectrum of CZG10 nanocomposite. The Figure shows the signals of C, Cu, Zn, O and Cr. The presence of C and Cu could be assigned from the carbon coated Cu grid used for the TEM measurement. In addition, the presence of rGO could also be the source of carbon. The existence of Zn and O elements could be due to the presence of ZnO and rGO forming CZG nanocomposite.

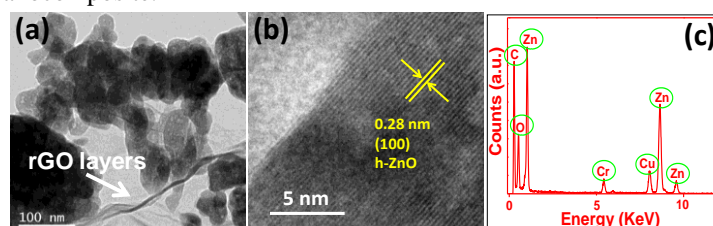


Fig. 2. FESEM images of (a) ZO and (b) CZG10 samples. TEM and HRTEM images of CZG10 nanocomposite are shown in (c) and (d), respectively. TEM SAED and TEM-EDS of CZG10 nanocomposite are displayed in (e) and (f), respectively.

4.1.3. FTIR spectra. Figure 3 displays the FTIR spectra of ZO, ZG, CZG2, CZG5, and CZG10 samples. The FTIR peaks appeared at 1732 , 1622 , 1208 and 1045 cm^{-1} in GO, attributed to COOH stretching vibration in carboxylic acid groups, the skeletal vibration of unoxidized graphitic domains as well as for the vibrations of C–O stretching, and C–OH stretching, respectively [2]. A prominent vibration appeared at $\sim 450 \text{ cm}^{-1}$ in ZO, ZG, CZG2, CZG5 and CZG10 nanocomposites, implying the presence of Zn–O stretching vibration of h-ZnO [7]. This observation strongly supported the XRD result (Fig. 1). A broad vibration appeared at $\sim 3440 \text{ cm}^{-1}$ in all the nanocomposites could indicate the presence of hydroxyl groups [2].

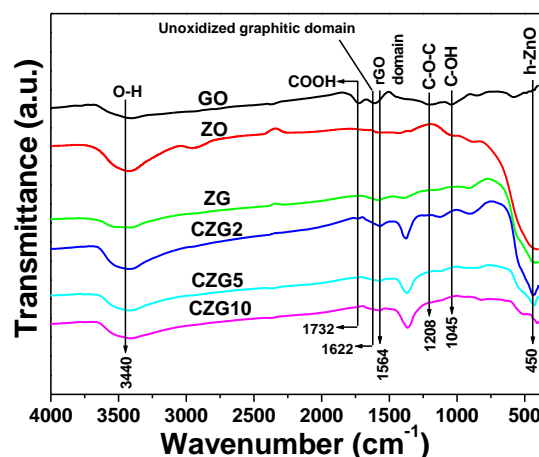


Fig. 3. FTIR spectra of ZO, ZG, CZG2, CZG5 and CZG10 samples along with as-synthesized graphene oxide (GO).

Moreover, the transformation of GO to rGO in GO loaded samples such as ZG, CZG2, CZG5, and CZG10 could be confirmed from the observation of a new peak at $\sim 1564\text{ cm}^{-1}$. It was worthy to note that this $\sim 1564\text{ cm}^{-1}$ vibration was also absent in pristine graphene oxide. Moreover, the FTIR vibrations responsible for oxygen functional groups of GO became very weak or nearly disappeared in the ZG, CZG2, CZG5 and CZG10 nanocomposites. The result further confirmed the transformation of GO to rGO in the nanocomposites.

4.1.4. Raman spectra. To understand the presence of structural defects/layer by layer exfoliation/chemical interaction of graphene in the nanocomposites with respect to the precursor GO, micro-Raman spectral study (Fig. 4) was carried out on GO, ZG and CZG10 nanocomposites. Two distinct Raman peaks were observed in each sample at $\sim 1350\text{ cm}^{-1}$ and at $\sim 1595\text{ cm}^{-1}$, assigned to D band (defect) and G (graphene) band, respectively [2]. Exfoliation/breaking of graphene layers could be the reason behind the origin of the D band whereas the source of G band (graphene) could be due to the presence of E_{2g} phonon in sp^2 carbon atoms of graphene moiety. The intensities of D and G bands were designated as I_D and I_G , respectively. The ratio of I_D/I_G was proved to be an important tool for understanding the chemical interaction that happened between rGO and the inorganic moiety (ZnO/Cr doped ZnO). The I_D/I_G value was much higher in ZG compare of ZO. This relative increment of I_D/I_G value could be accounted for the decrease of in-plane sp^2 domain size of graphene which could result in layer by layer exfoliation/breaking of graphene layers due to chemical interaction / complexation with the inorganic moiety [2]. Removal of oxygen functional groups due to the reduction/transformation of GO to rGO could also reflect through the increase of I_D/I_G value. Moreover, a further increment in I_D/I_G was also seen in CZG10 nanocomposite confirming the doping effect of Cr [3]. This increment of I_D/I_G ratio and the interaction between ZnO and rGO could be expected to enhance antibacterial activity of the material (discussed later).

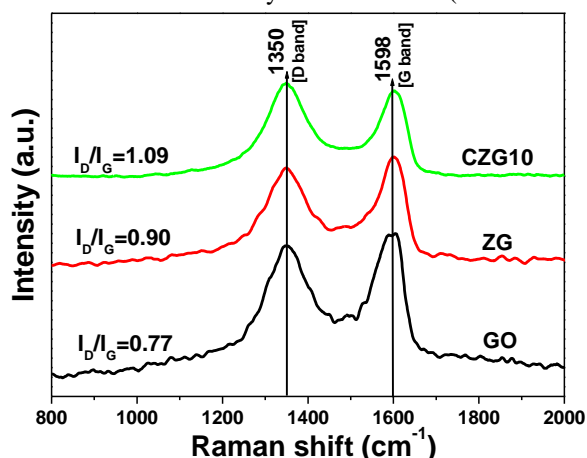


Fig. 4. Raman spectra of GO, ZG and CZG10 samples. Respective I_D/I_G value is embedded in the figure.

4.1.5. UV-Vis spectra. The optical properties of ZO, ZG, CZG2, CZG5 and CZG10 nanocomposites were investigated by UV-Vis absorption spectral study (measured by diffused reflectance method) (Fig. 5). The absorption spectra were obtained from the reflectance spectra of the samples with the help of Kubelka–Munk algorithm. As can be seen from the figure that a typical UV

absorption peak appeared at 360 nm, would be associated with the HOMO-LUMO transition of ZnO semiconductor [2]. The reason behind this transition in ZnO could be attributed to the electron transition from valence band to conduction band, related to the intrinsic band-gap of ZnO semiconductor [2]. It is also noted that the absorption peak was found to be shifted towards lower wavelength region in ZG and Cr doped ZG samples compared to pristine ZnO. Moreover, the visible light absorption seemed to be significantly enhanced with increasing chromium concentration in the precursor solution for obtaining chromium doped ZG nanocomposites (CZG). This shifting would be associated with the decrease in particle size of ZnO. On the other hand, a systematic enhancement in visible light absorption could possibly due to the effect of Cr-doping [1]. This visible light absorption could favour for obtaining better antibacterial activity of the material (discussed later).

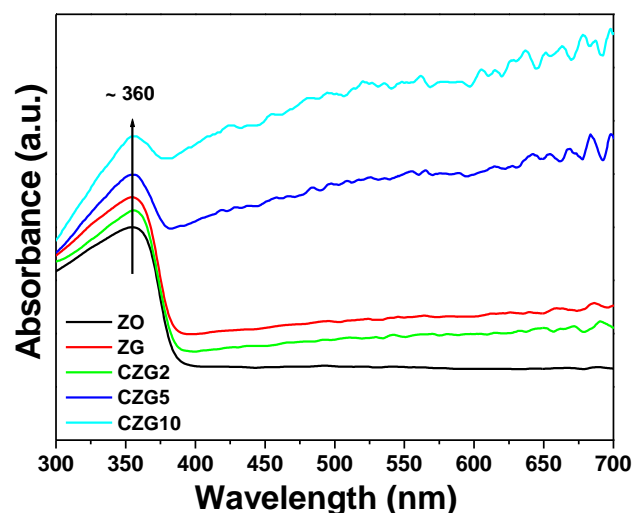


Fig. 5. Absorption spectra of ZO, ZG, CZG2, CZG5 and CZG10 samples.

4.2 Biomedical properties

4.2.1. Estimation of Minimum Inhibitory Concentration (MIC) nanocomposites. Gram-positive bacteria - *Staphylococcus aureus*, *Bacillus subtilis*, and Gram-negative bacteria – *Escherichia coli*, *Pseudomonas aeruginosa* was used as model microorganisms. Figure 6 shows the antibacterial activity of ZO, ZG, CZG2, CZG5 and CZG10 nanocomposites with different concentrations on *Staphylococcus aureus*, *Bacillus subtilis*, *Escherichia coli* and *Pseudomonas aeruginosa*. The figure clearly demonstrates the concentration dependent bacterial growth inhibition by Cr doped ZG nanocomposites. In this respect, the CZG5 nanocomposite has shown most effective antibacterial activity towards all the organisms. The MIC value for Gram negative bacteria (*Escherichia coli*, *Pseudomonas aeruginosa*) (Fig. 6a) and Gram positive bacteria (*Staphylococcus aureus* and *Pseudomonas aeruginosa*) (Fig. 6b) after the treatment of CZG5 nanocomposite were $3.125\text{ }\mu\text{g/ml}$ and $6.25\text{ }\mu\text{g/ml}$, respectively. From the Figure, it is revealed that the ZG nanocomposite seemed to have greater bacterial growth inhibition than ZO. Therefore, the rGO incorporation might have a negative influence on the bacterial growth. It is worthy to mention that rGO has the ability to kill bacterial cells by disrupting cell wall [10]. It also helps ZnO nanoparticles to enhance the antibacterial activity [2]. However,

doping Cr into the ZG nanocomposite, the inhibition of bacterial growth seemed to have taken greater leaps towards the antibacterial activity of the material. Moreover, the inhibition property seemed to increase with increasing Cr doping concentration in the precursors.

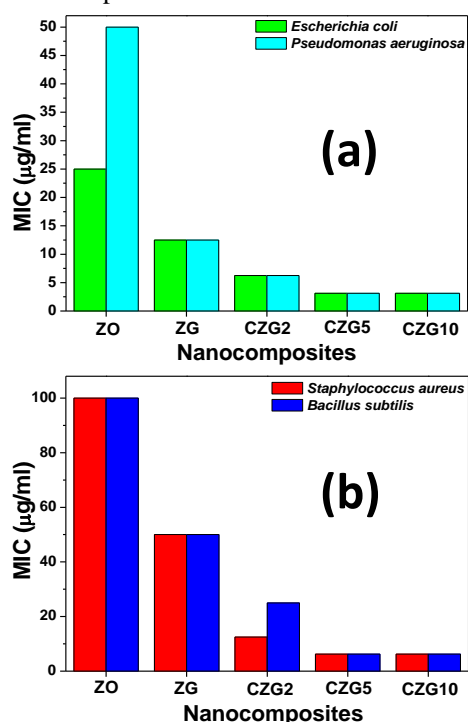


Fig. 6. Antibacterial activity of ZO, ZG, CZG2, CZG5, and CZG10 on (a) Gram negative and (b) Gram positive bacteria.

The proper mechanism of the antibacterial activity of nanomaterials including nanocomposite is not yet known in a

distinct manner. However, probable mechanisms of nano ZnO had been discussed in our previous report [2]. On this aspect, the incorporation of Zn^{2+} into the bacterial cell membrane and the accumulation of nanoparticles could be the reason for the death of the bacterial cells [2,11]. The destruction of cell membrane also could result in leakage of minerals, proteins and genetic materials which eventually cause the cell death [2,12]. In the present work, the enhanced bacterial growth inhibition of Cr doped ZG nanocomposite (CZG) could be associated with the shifting of visible light absorption and the presence of defects [1] as revealed from Figure 5. This would enforce the creation of more reactive oxygen species (ROS) generation compared to nano ZnO [1] towards enhancement in antibacterial activity of the material. Another reason could be the enhanced interaction between ZnO and rGO (Fig. 4, Raman spectra) which would generate more ROS and eventually more bacterial cell death. Zn^{2+} ions would also occupy in the interstitial position, due to the successful substitution of some Zn^{2+} ions by Cr^{3+} ions into ZnO lattice (Fig. 1). This would result in the release of Zn^{2+} ions from ZnO lattice. Therefore, the simultaneous release of Zn^{2+} and Cr^{3+} ions would cause in enhancing antibacterial activity of the material [1]. The reduction in crystallite size due to the Cr^{3+} ions incorporation would also have an effect upon the antibacterial activity. The smaller crystallite sized nanoparticle would enter into the bacterial cell and inhibit DNA replication as well as protein synthesis which would cause the death of bacterial cells [2]. This reason seemed to apt with CZG10 nanocomposite as the crystallite size was less than the other nanocomposites, showing better inhibition to the growth of bacteria than the other nanocomposites.

5. CONCLUSION

In summary, for the first time, we synthesized Cr doped ZnO-rGO nanocomposites with highly effective antibacterial activity at room temperature in presence of hydrazine hydrate. A series of Cr doped-ZnO-rGO nanocomposites were synthesized by changing the chromium loading concentration in the precursors. The as-synthesized nanocomposites show an excellent antibacterial activity compares to pristine ZnO nanoparticles towards Gram negative and Gram positive bacteria. The 5% Cr doped nanocomposite exhibits the best antibacterial activity as the

nanocomposite which is able to inhibit the bacterial growth at 6.25 and 3.125 $\mu\text{g/ml}$ for Gram-positive bacteria - *Staphylococcus aureus*, *Bacillus subtilis*, and Gram-negative bacteria - *Escherichia coli*, *Pseudomonas aeruginosa*, respectively. Therefore, Cr incorporation in ZG nanocomposite seems to have an enhanced capability to inhibit the growth of bacteria than ZG nanocomposite. This synthesis strategy can open an avenue in other metal oxide doped ZG nanocomposites for the biomedical application.

6. REFERENCES

- [1] Vijayalakshmi K., Sivaraj D., Enhanced antibacterial activity of Cr doped ZnO nanorods synthesized using microwave processing *RSC Adv.*, 5, 68461–68469, 2015.
- [2] Naskar A., Bera S., Bhattacharya R., Saha P., Roy S.S., Sen T., Jana S., Synthesis, characterization and antibacterial activity of Ag incorporated ZnO–graphene nanocomposites, *RSC Adv.*, 6, 88751–88761, 2016.
- [3] Naskar A., Khan H., Jana S., Cobalt doped ZnO-graphene nanocomposite: Synthesis, characterization and antibacterial activity on water borne bacteria, *AdvNanoBioM&D*, 1, 4, 182-190, 2017.
- [4] Mary J.A., Vijaya J.J., Kennedy L.J., Bououdina M., Microwave-assisted synthesis, characterization and antibacterial properties of Ce–Cu dual doped ZnO nanostructures, *Optics*, 127, 2360-2365, 2016.
- [5] Shah A.H., Ahamed M.B., Neena D., Mohammed F., Iqbal A., Investigations of optical, structural and antibacterial properties of Al-Cr dual-doped ZnO nanostructures, *J Alloys Compd.*, 606, 164-170, 2014.
- [6] Naskar A., Bera S., Bhattacharya R., Roy S.S., Jana S., Effect of bovine serum albumin immobilized Au-ZnO-graphene nanocomposite on human ovarian cancer cell, *J Alloys Compd.*, 734, 66-74, 2018.
- [7] Naskar A., Bera S., Bhattacharya R., Roy S.S., Jana S., Synthesis, characterization and cytotoxicity of polyethylene glycol coupled zinc oxide–chemically converted graphene nanocomposite on human OAW42 ovarian cancer cells, *Polym. Adv. Technol.*, 27, 436-43, 2016.
- [8] Bera S., Naskar A., Pal M., Jana S., Low temperature synthesis of graphene hybridized surface defective hierarchical core–shell structured ZnO hollow microspheres with long-term stable and enhanced photoelectrochemical activity, *RSC Adv.*, 6, 36058–68, 2016.
- [9] Bera S., Pal M., Naskar A., Jana S., Hierarchically structured ZnO-graphene hollow microspheres towards effective reusable adsorbent for organic pollutant via photodegradation process, *J. Alloys Compd.*, 669, 177–86, 2016.
- [10] Xie X., Mao C., Liu X., Zhang Y., Cui Z., Yang X., Yeung K.W.K., Pan H., Chu P.K., Wu S., Synergistic bacteria killing through

photodynamic and physical actions of graphene oxide/Ag/collagen coating, *ACS Appl. Mater. Interfaces*, 9(31), 26417-26428, **2017**.

[11] Đolić M.B., Rajaković-Ognjanović V.N., Štrbac S.B., Dimitrijević S.I., Mitrić M.N., Onjia A.E., Rajaković L.V., Natural sorbents modified

by divalent Cu²⁺- and Zn²⁺- ions and their corresponding antimicrobial activity, *New Biotechnol.*, 39, 150-159, **2017**.

[12] Wang L., Hu C., Shao L., The antimicrobial activity of nanoparticles: present situation and prospects for the future, *Int J Nanomedicine*, 12, 1227–1249, **2017**.

7. ACKNOWLEDGEMENTS

One of the authors, AN thankfully acknowledge UGC-RGNF for providing his Ph.D. research fellowship. Authors also thankfully acknowledge the help of Mr.Trivid Sarkar, Department of Pharmaceutical Technology, Jadavpur University, India for his help to measure the antibacterial activity of the materials. The authors also acknowledge the help rendered by Nanostructured Materials Division and Bioceramic and Coating Division as well as Electron Microscopy Section for several characterizations. The work had been done as an associated research work of 12th Five Year Plan project of CSIR (No. ESC0202).

© 2018 by the authors. This article is an open access article distributed under the terms and conditions of the Creative Commons Attribution license (<http://creativecommons.org/licenses/by/4.0/>).